Renewable Energy 244 (2025) 122684

Contents lists available at ScienceDirect

Renewable Energy

journal homepage: www.elsevier.com/locate/renene

Impact of thermoelectric coal-fired power plant emissions on the soiling mechanisms of nearby photovoltaic power plants in the Atacama Desert

D. Olivares [a,*], A. Marzo [b,c,**], A. Taquichiri [a], R. Espinoza [a], M. Henriquez [a], C. Portillo [a], P. Ferrada [d], L.A. Conde [e], E. Fuentealba [a], V. del Campo [f,g]

[a] Centro de Desarrollo Energético Antofagasta, Universidad de Antofagasta, Angamos 601, Antofagasta, 1270300, Chile
[b] Department of Optics, University of Granada, Profesor Adolfo Rancaño St, 18071, Granada, Spain
[c] CIESOL, Joint Centre of the University of Almería-CIEMAT, 04120, Almería, Spain
[d] Materials and Sustainability Group, Department of Engineering, Universidad Loyola Andalucía, Avda. De las Universidades s/n, Dos Hermanas, 41704, Seville, Spain
[e] Solar Energy Research Center, Universidad de Chile, Tupper 2007, 8370451 Santiago, Chile
[f] Departamento de Física, Universidad técnica Federico Santa María, Av. España 1680, Valparaíso, Chile
[g] Millenium Nucleus in NanoBioPhysics (NNBP), Av. España 1680, Valparaíso 11520, Chile

ARTICLE INFO

Keywords:
Soiling
Photovoltaic
Cementation
Physicochemical analysis
Thermoelectric coal-fired power plant

ABSTRACT

Soiling of photovoltaic modules is a problem that causes production and economic losses and is highly dependent on local environmental conditions. Photovoltaic plants' operators need to develop operation and maintenance strategies to balance the investment in cleaning procedures with these economic losses, especially in industrial areas. This paper analyses the impact of coal-fired power plants on the soiling mechanisms in photovoltaic plants in Atacama Desert. For that, the accumulated dust on the modules and its effect on the PV plant performance is analysed and compared in three different places in Atacama Desert. Two of them are in the coastline, one close to thermoelectric coal-fired power plant and another in the inner desert. The adhesion mechanism of deposited material and the impact of soiling on energy generation in photovoltaic modules installed within the coal-fired power plant are analysed. Our results show that calcite, used in the sulphur gas reduction process at the power plant, generates synthetic gypsum (FDG), which facilitates dust cementation on photovoltaic modules. Furthermore, our results indicate that the effects of the power plant's activity are noticeable up to 9 km away, becoming particularly evident in areas with high humidity, where the solubility of materials enhances the recrystallization and consolidation of dust on module surfaces. Specifically, the impact of the coal-fired power plant on the modules installed within its premises shows that after five months of exposure, the deposited dust reaches a maximum of 1.63 mg/cm^2, with a soiling rate up to six times higher compared to other studied locations, resulting in a 23 % reduction in photocurrent.

1. Introduction

Global energy generation is a very attractive investment for the stock market. Over the last century, it has been mainly based on fossil fuels due to their low production costs, economic profitability, and lack of other economically competitive energy sources. However, in recent decades there has been increasing evidence of their detrimental impact on the environment, global climate and human health [1]. Renewable energy technologies are competitive in the electricity market and provide a solution to environmental challenges, promoting a sustainable development. This was demonstrated in 2020 when renewable energy sources overtook fossil fuels in the European Union electricity sector for the first time [2]. In this sense, solar photovoltaic (PV) has emerged as a clean and competitive alternative in the global energy market [3–6].

The attractive benefits of PV projects are mainly related to their profitability, which must consider both the income generated by the plant's production and the costs associated with the initial investment (CAPEX) and the operation and maintenance (OPEX). Usually, the initial investment is high, but OPEX can reach 60 % of the total investment during the lifetime of the PV system [7]. The technological and industrial development in recent decades, especially with the entry of China into the market, have resulted in a reduction of PV modules' costs and,

* Corresponding author.
** Corresponding author. Department of Optics, University of Granada, Profesor Adolfo Rancaño St, 18071, Granada, Spain.
E-mail addresses: douglas.olivares@uantof.cl (D. Olivares), aitorm@ugr.es (A. Marzo).

https://doi.org/10.1016/j.renene.2025.122684
Received 6 August 2024; Received in revised form 1 February 2025; Accepted 15 February 2025
Available online 18 February 2025
0960-1481/© 2025 The Authors. Published by Elsevier Ltd. This is an open access article under the CC BY license (http://creativecommons.org/licenses/by/4.0/).

consequently, in the construction costs of PV plants [8]. However, to take full advantage of a photovoltaic installation, external factors related to geographical and environmental conditions must be determined. Local environmental conditions, such as the amount of available solar resource and its spectral distribution, as well as soiling properties and deposition rate, determine plant energy conversion and losses in production [9–17]. According to a study presented by Ilse et al. [18], in an optimal cleaning scenario, dirt reduces at least 3 %–4 % of the world's solar energy production, with losses exceeding 3 billion euros annually. However, soiling is a condition which can be addressed through an operation and maintenance plan designed accordingly with the environmental conditions [19].

Cleaning and maintenance strategies are essential for photovoltaic (PV) power plants as soiling, caused by the accumulation of dust and dirt on module surfaces [14,20–23], can significantly reduce efficiency and energy output, leading to economic losses [18,24]. This underscores the urgency of research to optimise cleaning processes, mitigate the impacts of soiling and site selection [18,24].

Efficient operation and maintenance (O&M) costs require strategies such as manual or automated cleaning systems and anti-soiling coatings, balancing cleaning costs with energy gains [24]. Furthermore, improper cleaning methods or excessive soiling can damage module surfaces, reducing their lifespan. Gentle and appropriate cleaning techniques help preserve the durability of PV modules [18]. Understanding the mechanisms and characteristics of soiling is therefore critical to develop effective prevention, cleaning, and maintenance strategies suited to local conditions.

Local environmental conditions significantly influence soiling dynamics, directly affecting the performance of PV systems [24,25]. Industrial activity is an additional contributor, generating pollutants that deposit on module surfaces and exacerbate soiling issues [24,26]. Climatic and meteorological conditions play a decisive role in soiling deposition. Monitoring systems are crucial for assessing soiling levels, optimising cleaning schedules, and predicting when cleaning is needed [25,27]. Research has focused on monitoring methods, frequency optimisation [25], and cost-effective soiling mitigation strategies, emphasising the need to adapt to specific climates [18,24]. Arid and semi-arid regions, characterised by high solar irradiance and abundant airborne particulates, are especially prone to dust accumulation [12,28–31]. Dust storms and prolonged dry periods further increase the risk of soiling, while the scarcity of rainfall limits natural cleaning processes. Wind speed and direction influence the transport and deposition of dust, although their effects vary depending on the specific particle characteristics in the area [25]. Relative humidity and the tilt angle of the PV modules are also critical factors. While rainfall can help clean modules, it may leave behind sticky residues when combined with certain contaminants [15,24–26]. The nature of the dust itself, including its size, chemical composition, and density, is equally important in determining its impact on PV performance [29,30]. Fine particles, for example, tend to distribute more uniformly across module surfaces and may result in greater performance losses compared to larger particles [32]. Moreover, the chemical composition of dust varies widely by geographical location, affecting both its adhesion properties and the difficulty of removal [28]. Geographical factors add further complexity, as soiling is inherently site-specific and subject to temporal and spatial variability [30]. Even within the same PV plant, differences in soiling can arise due to microclimatic conditions or proximity to localised sources of dirt. In tropical regions, the combination of low module tilt angles and high particulate deposition often results in increased soiling rates [33]. In contrast, arid regions like Qatar have reported soiling losses exceeding 10 % [34], while in the Atacama Desert, annual energy losses due to soiling have been observed to reach up to 35 % in coastal areas [35,36]. These efforts highlight the importance of cleaning and maintenance to ensure the efficiency, reliability, and profitability of PV power plants [18,27].

Industrial activity significantly contributes to soiling by introducing a variety of contaminants into the environment. Emissions from factories and motor vehicles deposit soot, hydrocarbons, and other pollutants onto PV module surfaces [26]. In urban and industrialised areas, the soiling layer often contains a mixture of fine particulates, combustion residues, and sticky substances formed through interactions with humidity [27,33]. These contaminants are especially challenging to remove and may require advanced cleaning strategies. In addition to industrial emissions, other sources of soiling include the proximity to loose soils, agricultural activities, pollen, bird droppings, and microbial colonisation [37,38]. In tropical climates, biosoiling by microorganisms can substantially degrade the efficiency of PV modules over time [37]. Furthermore, the heterogeneity of soiling sources within a given location underscores the need for tailored mitigation strategies.

The global transition to renewable energy has driven coal power plant operators to explore ways to integrate solar technologies into their existing infrastructure. While this shift cannot occur overnight, many coal power developers are initiating the deployment of solar photovoltaic (PV) systems as a complementary technology to operate alongside coal-fired plants until the latter reach the end of their economic lifetime. Hybrid solar-coal power plants have relied on concentrating solar power (CSP) technologies, also known as solar thermal [39–44]. However, recent projects increasingly incorporate solar PV modules due to their cost-effectiveness and scalability. The integration of solar PV with coal-fired power plants offers a promising path to improve the operational stability of renewable energy systems and reduce fossil fuel consumption, while also leveraging the existing infrastructure [45]. By combining the advantages of solar PV—clean and intermittent energy—with the dispatchable nature of coal power, hybrid plants can ensure a more efficient and sustainable electricity generation process [46,47]. These systems allow for the optimisation of resources, reducing the carbon footprint of coal plants while transitioning toward renewable energy.

However, coal-fired power plants are significant sources of atmospheric pollution, emitting particulates such as soot and inorganic pollutants alongside gases like carbon monoxide (CO), sulphur dioxide (SO_2), and nitrogen oxides (NO_x) [48,49]. To reduce these emissions, control technologies such as flue gas desulfurization, selective catalytic reduction and particulate filters are used to capture and reduce these pollutants. However, these technologies produce pollutant by-products such as fine particulate matter (PM2.5) and coarse particulate matter (PM10). The deposition of combustion by-products, such as fine particulate matter and soot, can form dense layers on solar panels, limiting the transmission of sunlight to the cells and degrading energy output [48,49]. While the feasibility of hybrid solar-coal systems has been explored in terms of operational efficiency and environmental benefits, studies addressing the impact of industrial emissions from coal combustion on soiling mechanisms and O&M cost are, to the best of our knowledge, notably absent from the literature.

The present study addresses this gap by analysing the soiling mechanisms on a PV plant located within the vicinity of a conventional coal-fired power plant. To achieve this, we characterised the physical, chemical, and morphological properties of the material deposited on PV modules. These findings were compared with soiling levels observed at three other PV plants situated 9 km, 60 km, and 120 km away from the coal plant. Additionally, the study evaluated the impact of soiling from the coal-fired plant on solar energy production. Over a 24-week monitoring period, we assessed the mass density of deposited dust, changes in the optical properties of the glass surface, and the photogenerated current of conventional PV modules. The results provide critical insights for researchers and PV plant operators, offering guidance on mitigation strategies and cleaning plans for installations under similar environmental conditions.

2. Methodology

2.1. Location

This study was primarily conducted in the city of Mejillones (23.09° S, 70.41° E), a coastal locality classified as BWk according to the Köppen-Geiger climate classification [50], identifying it as an arid zone with a cold-temperate climate [51]. Mejillones is characterized for hosting the largest concentration of coal-fired power plants in Chile, with a total of 8 units and an installed capacity of 1800 MW. Within one of these coal-fired power plants is the PV plant under study, highlighted in green in Fig. 1a. This facility has a capacity of 21.6 kW and consists of commercial multicrystalline silicon modules. Designed with a northward orientation and a tilt angle of 25°, the photovoltaic plant was conceived to supply electrical energy to work areas, lighting, and low-power equipment. In this facility, the impact of the coal-fired power plant on soiling mechanisms and effects in PV plant was analysed. The importance of studying soiling in the city of Mejillones lies in its abundant solar resource, with annual values exceeding 2500 kWh/m^2. These conditions have enabled the city to host approved and under-construction photovoltaic projects with a total net capacity of 573 MW [52].

To establish the effect of the coal-fired power plant on soiling, the results obtained at Mejillones were compared with those of three other sites in the Atacama Desert. The first corresponds to a PV plant located 9 km away, identified as Site 2 and marked in blue in Fig. 1a). This PV plant has a net capacity of 370 MW and is located close to three coal-fired power plants, which are marked in purple in the same figure. The other two study sites, although far from the direct impact of the coal-fired power plant, share the same climate as Mejillones (BWk): the city of Antofagasta and the Plataforma Solar del Desierto de Atacama (PSDA). The city of Antofagasta (23.70°S and 70.42°W) is a coastal town similar to Mejillones, located 60 km to the south. Both cities have minimal rainfall and are influenced by the Pacific Ocean [53]. The PSDA (24.09°S and 69.93°W) is an open-air facility dedicated to the study and testing of solar technologies, located in the interior of the desert, 120 km from Mejillones. With an altitude of 963 m above sea level, this area corresponds to a cold and arid desert classified as BWk [54]. Both locations represent characteristic scenarios of the Atacama Desert for the development of photovoltaic projects. Fig. 1b) shows a satellite image of the three locations: Mejillones (green circle), Antofagasta (red circle) and the PSDA (orange circle).

2.2. Instrumentation and methods

Dust samples were taken from the PV system located at the coal-fired power plant facilities in Mejillones and at the PV plant defined as site 2 (Fig. 1a green and blue). Samples were collected with a soft bristle brush, brushing from top to bottom to remove all deposited material. To obtain greater representativeness, a composite sample was generated for each module chain, which were subsequently processed with a rotary micro riffler (Quantachrome). This device uses mechanical energy (vibration) to produce constant flows of material from the composite powder, separating the material to reduce segregation and improve representativeness. From this process, a final composite sample was obtained for chemical and morphological characterization of both sites.

The chemical characterization was performed at room temperature using a Bruker AXS D8 Advance X-ray diffractometer (XRD) in the 5-70° range, with a CuKα (λ = 0.15045pm) lamp at 40 kV and 30 mA. The PDF-4 database [55] was used to detect the crystalline species present in the sample. Semi-quantification of the crystalline species was performed using TOPAS software, which uses the Rietveld method to determine the abundance of the crystalline species based on signal intensity [56]. Additionally, a detailed characterization of the dust particles was performed through scanning electron microscopy (SEM) and energy-dispersive X-ray spectroscopy (EDX) with a Joel SEM model JSM-6360 LV.

The morphological analysis was carried out using a Leica optical microscope model DM IRB that includes a size bar. Images were taken at a magnification of 20x and analysed using ImageJ software [57]. The

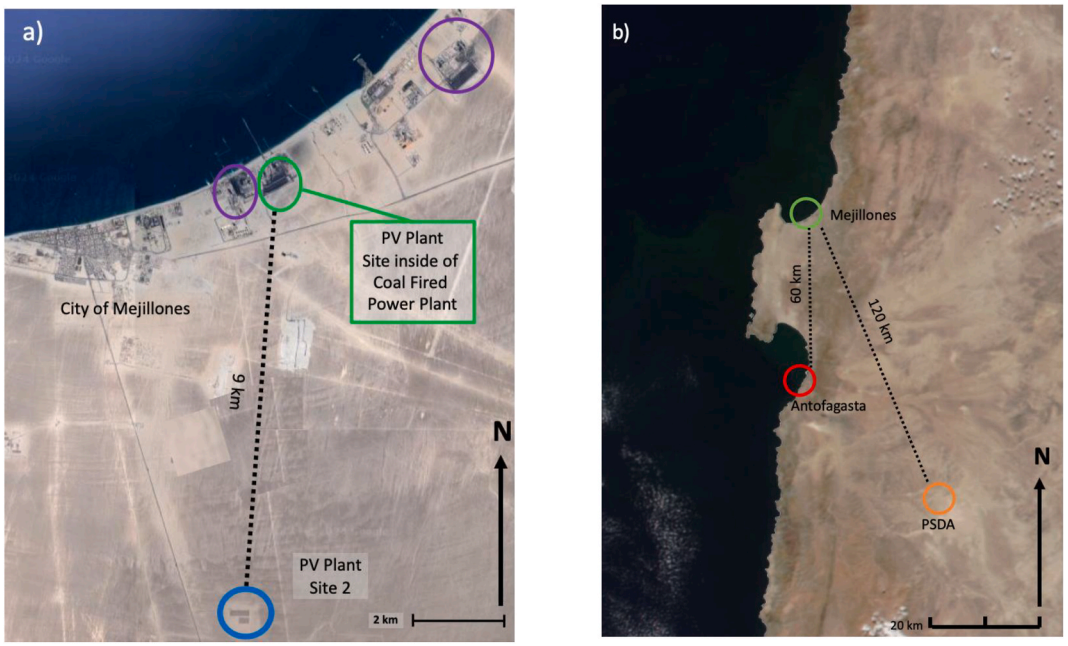


Fig. 1. a) Map showing the location of coal-fired power plants in the city of Mejillones. The coal-fired power plant where the photovoltaic plant under study is installed is highlighted in green. Two additional operational coal-fired power plants in the area are marked in purple(https://www.google.com/maps). b) Image taken from the website of the Aeronet PSDA_Chile weather station (https://aeronet.gsfc.nasa.gov/). The image corresponds to a capture made by the Terra_MODIS satellite on March 22, 2023. The figures on the right show the details of the corresponding locations. The red circle highlights the location of the photovoltaic plant installed in the city of Mejillones, the green circle marks the position of the city of Antofagasta, and the orange circle marks the location of the Plataforma Solar del Desierto de Atacama. (For interpretation of the references to colour in this figure legend, the reader is referred to the Web version of this article.)

geometrical parameters for each particle (longest projection and shape factor) were obtained from the software: area (A), perimeter (P), and aspect ratio (C_τ) as follows. The roundness coefficient [58]is defined as:

$$R = \frac{A}{A_{Fmax}} \tag{1}$$

where A corresponds to the particle area, and A_{Fmax} to the area of the circle with a diameter equals to maximum Feret value given by:

$$A_{Fmax} = \frac{\pi d_{Fmax}^2}{4} = \frac{\pi l^2}{4} \tag{2}$$

Where d_{Fmax} is the particle's longest projection, to be named l in this work for clarity purposes.

Then, the roundness coefficient is given by equations (1) and (2) is defined by:

$$R = \frac{4A}{\pi l^2} \tag{3}$$

At the same time, the roundness coefficient corresponds to the inverse the aspect ratio (C_τ):

$$C_\tau = \frac{1}{R} = \frac{\pi l^2}{4A} \tag{4}$$

Since C_τ and A are parameters obtained from ImageJ, we use them to compute the longest projection:

$$l = \sqrt{\frac{4AC_\tau}{\pi}} \tag{5}$$

The morphology of the deposited material was analysed using the shape factor (A_{Shape}). This parameter is associated to the geometrical complexity and was used by Aissa et al. [59]in their study about dust particles in Qatar and their influence on the PV panel performance. The shape factor is calculated through Eq. (2), where P and A are the particles' perimeter and area, respectively. A shape factor closes to 1 corresponds to a perfect circle. For this test, around 400 particles were analysed to ensure the representativeness of the result.

$$A_{Shape} = \frac{P^2}{4\pi A} \tag{6}$$

To quantify the amount of deposited material, 46 standard PV glass samples (25.4 mm × 76.2 mm), without anti-soiling coatings, were installed with a north orientation and a 20° tilt on the surface of the PV modules. Two samples were weekly removed for 5 months (from September 21st, 2022, to March 2nd, 2023) and weighed using a precision balance from A&D HR. Additionally, to characterize soling effect on the optical properties of PV glasses, each dusted glass was placed on a monocrystalline silicon irradiance sensor (Silicon Irradiance Sensor Si-V-10TC), which response was compared to one with a clean glass. The experimental setup can be observed in Fig. 2. These sensors were kept with north orientation, and with an appropriate inclination to obtain the maximum value at solar noon. The samples were placed on the sensors in the morning and removed at dusk to ensure that there was no condensation effect from the environment. The data obtained from two days of optical measurements were collected using a Campbell Scientific CR1000X datalogger.

Theoretical photogenerated current was computed through Eq. (7) and integrated between 300 and 1200 for a standard PV cell. The initial photocurrent density ($J_{ph,clean}$) was determined from the ASTM AM1.5G reference spectrum (ϕ_{in}), and the external quantum efficiency (EQE) data reported previously for a standard p-type solar cell [14]. Subsequently, the photogenerated current density under soiled conditions was obtained by applying the transmittance loss due to soiling (τ_{loss}) using Eq. (8).

$$J_{ph,clean} = \frac{q}{h\,c} \int_{\lambda_o}^{\lambda_g} \phi_{in}(\lambda)\, EQE(\lambda)\, \lambda\, d\lambda \tag{7}$$

$$J_{ph} = \left(1 - \frac{\tau_{loss}}{100}\right) J_{ph,clean} \tag{8}$$

To determinate the atmospheric parameters involved in the soiling process of the modules installed in the coal-fired power plant, the data was obtained from the General Directorate of Civil Aeronautics who operates the meteorological station located in the city of Mejillones (−23.10917°, −70.44333°) [60]. Their records include daily, monthly, yearly, and historical datasets, drawing upon information sourced from various official channels of the Chilean Meteorological Directorate. Among which are the SACLIM systems databases, the network of automatic stations, and the information transmitted through the AFN network. For the purposes of this study, we specifically analysed data related to wind speed and direction (W_s and W_d), relative humidity (Rh), and ambient temperature (T_a) from September 1, 2022, to February 28, 2023.

3. Results and discussion

3.1. Physicochemical analysis

The results obtained by XRD of the dust deposited on the surface of the photovoltaic modules in the city of Mejillones are shown in Fig. 3. The detected crystalline compounds correspond to: (a) calcite ($CaCO_3$),

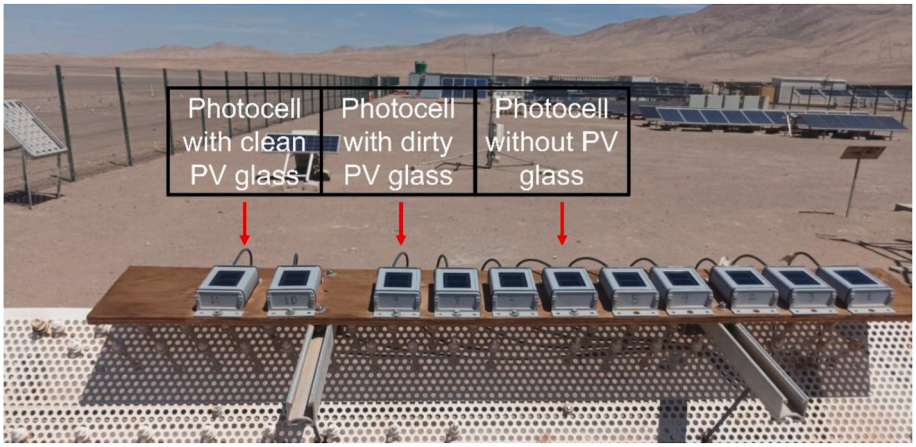


Fig. 2. Experimental setup for optical measurements of clean and dirty photovoltaic glass, utilizing irradiance SENSOR silicon. (For interpretation of the references to colour in this figure legend, the reader is referred to the Web version of this article.)

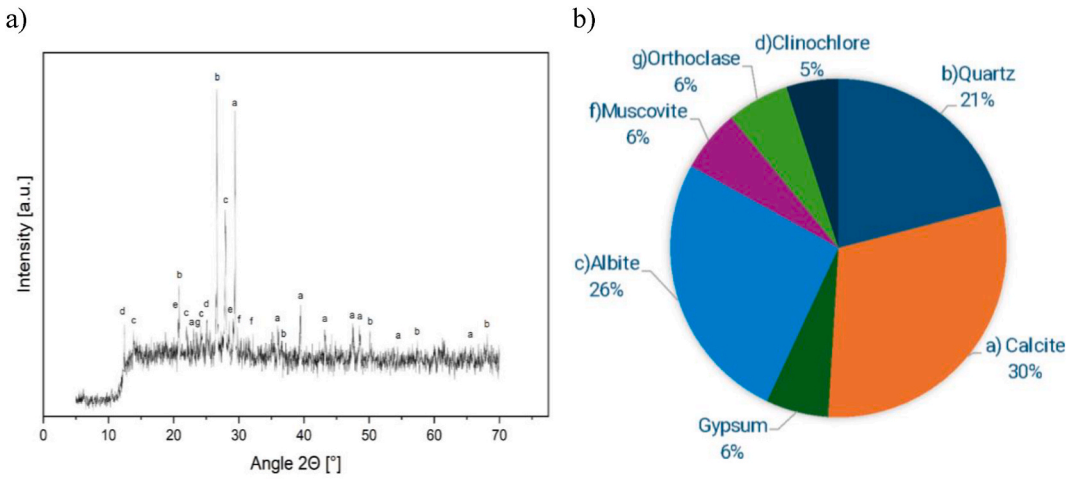


Fig. 3. a) X-ray diffraction (XRD) for sample of dust deposited on the surface of PV modules. The detected crystalline compounds correspond to (a) calcite ($CaCO_3$), (b) quartz (SiO_2), (c) albite ($Na(AlSi_3O_8)$), (d) clinochlore ($(Mg,Al,Fe)_6(Si,Al)4O_{10}(OH)_8$), (e) gypsum ($CaSO_4{\cdot}2H_2O$), (f) muscovite ($(H,K)AlSiO_4$), and (g) orthoclase ($KAlSi_3O_8$). b) Percentages of the compounds detected on the dust samples from the PV modules.

(b) quartz (SiO_2), (c) albite ($Na(AlSi_3O_8)$), (d) clinochlore ($(Mg,Al,Fe)_6(Si,Al)_4O_{10}(OH)_8$), (e) gypsum ($CaSO_4{\cdot}2H_2O$), (f) muscovite ($(H,K)AlSiO_4$), and (g) orthoclase ($KAlSi_3O_8$). It can be observed that mainly clays and silicates are present, which are in accordance with the geological composition of the area dominated by quartz and mafic [61]. Fig. 3b shows the concentration of crystalline species, obtained from the semi-quantitative analysis carried out using TOPAS. The analysis revealed the following fractions of deposited material: calcite (30 %), quartz (21 %), gypsum (6 %), albite (26 %), muscovite (6 %), orthoclase (6 %), clinochlore (5 %). The high levels of quartz are consistent with the coastal soil of the local geography [62]. Conversely, the high levels of calcite come from the thermoelectric coal-fired power plant, where it is extensively used to reduce sulphur dioxide (SO_2) emissions to the atmosphere [63]. The main advantage of using excessive calcite is to avoid the subsequent treatment of combustion gases.

The XRD analyses also revealed the presence of gypsum. This compound has soluble and hygroscopic properties that facilitate the cementation process on the surface of PV modules [20,64–66]. Regardless of the quantities of this compound, its presence, along with local atmospheric conditions, could induce the formation of cemented crusts. To confirm cementation and determine the soiling mechanism morphological and elemental characterizations were performed.

3.2. Morphological and structural analysis

For the morphological analysis, particles were separated between isolated and agglomerated. Fig. 4a shows the size distribution of all the deposited particles between 1 μm and 100 μm. The range below 100 μm includes 80 % of the analysed particles, which is consistent with reports from other authors for different locations [57,67,68]. Almost 80 % of this subset are smaller than 30 μm, while less than 5 % are above 60 μm. Both types of granules show the highest frequency for sizes between 10 and 20 μm, with a frequency of 44 % and 35 % for agglomerated and isolated grains respectively. The larger amount of agglomerated grains, compared to the isolated ones, below 20 μm could be an indication that very small particles tend to cluster more than those above 20 that size.

The morphological analysis was conducted using the shape factor (A_{Shape}), and the results are shown in Fig. 4b. The data reveal a low occurrence of spherical particles ($A_{Shape} \sim 1$), with a frequency of approximately 20 % for both isolated and agglomerated granules. Most of the particles, regardless of their state, exhibit a shape factor between 1.5 and 2, indicating a predominance of non-spherical geometries. The measured particles do not show a correlation between size and shape, however, the ~20 % presence of spherical grains is consistent with the frequencies of particles with sizes below 10 μm, which are 23 % and 25 % for agglomerated and isolated material, respectively [69,70].

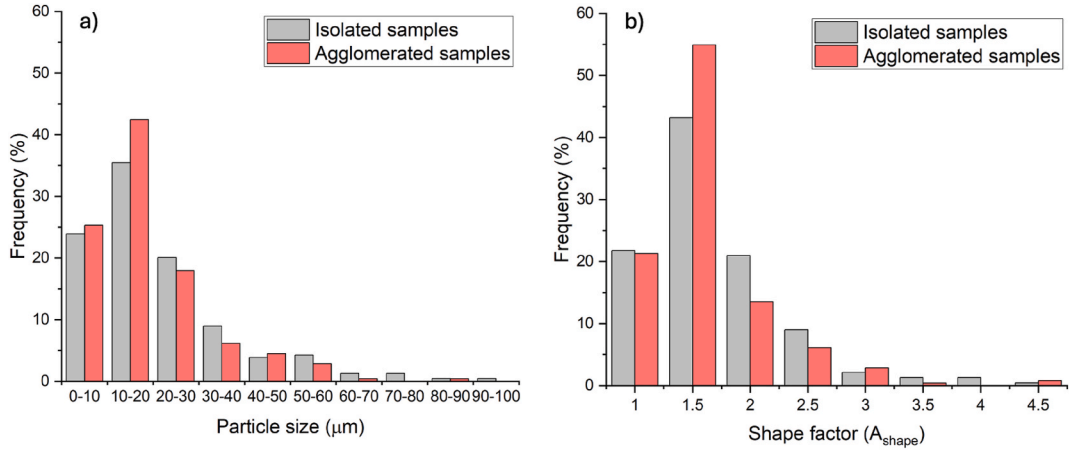


Fig. .4. a) Particle size distribution of dust deposited on the surface of PV modules. The grey bars correspond to agglomerated dust, while the red bars represent isolated samples; b) Particle shape factor distribution of agglomerated dust (red bars) and isolated samples (grey bars). (For interpretation of the references to colour in this figure legend, the reader is referred to the Web version of this article.)

As observed in the shape analysis, most of the deposited particles are far from being spherical. Prismatic particles (observed in SEM images in Fig. 5) correspond to gypsum, which crystallizes in a monoclinic system with prism-shaped crystals of rhombic form with beveled edges on the faces [56,57,65,68]. One of its main characteristics is the arrow-shaped or spear-shaped structure at one end, a phenomenon that can be clearly observed in Fig. 5 (a and b, marked in red). Additionally, the crystal structure of calcite, with a rhombohedral shape, further confirms the non-spherical nature of most of the deposited particles as observed in the shape analysis (Fig. 4b). The combined results of shape analysis and SEM observations are consistent with X-ray diffraction (XRD) results, which confirm a high abundance of calcite and significant amounts of gypsum in the deposited material. The correlation between chemical composition and particle morphology highlights the role of gypsum and calcite in the formation of accumulation dust patterns.

The elemental analysis by EDX is shown in Fig. 5(d and e and f), where the presence of magnesium, aluminium, sulphur, silicon, potassium, calcium, iron and sodium can be observed, in agreement with the results obtained by X-ray diffraction (XRD). In Fig. 5e, the abundant presence of silicon stands out, due to the geographical location of the site in a coastal zone. Meanwhile, Fig. 5f shows the combination of sulphur (in blue) and calcium (in pink) in the central particle, confirming its identification as gypsum. The EDX maps show how gypsum traps quartz crystals and other compounds to form compact agglomerates. This phenomenon is known as desert pavement or gypsum crust, a common feature in arid and desert environments [71], promoted by the interaction of atmospheric elements, such as moisture and evaporation cycles, with the geological components of the environment. Fig. 5e and f also highlight the presence of calcium, which is attributed to calcite, a mineral identified as one of the main fouling components in the PV plant installed in the coal-fired power plant. Calcite, like gypsum, plays a central role in the formation of cemented crusts due to its ability to partially dissolve under high humidity conditions. To study the formation of desert pavement crusts caused by gypsum or cementation resulting from calcite, we analysed local atmospheric conditions, including temperature, relative humidity, and wind speed and direction [66,72,73].

Fig. 6 depicts the behavior of atmospheric conditions over the course of the 6-month experimentation period. Ambient temperature (Fig. 6a) shows the seasonal change from spring to summer through a positive slope. In spring the average temperature is 17 °C with a minimum of 7 °C (September 2022); while the average in summer is 22 °C with a maximum of 31 °C (February 2023). Relative humidity (RH) shows values between 38 % and 94 % in spring and between 34 % and 92 % in summer (Fig. 6b). These high values observed for both seasons are influenced by the Pacific Ocean due to its geographical location. It is also noticeable that during spring, relative humidity is higher compared to summer. Lastly, wind speed and direction, depicted in Fig. 6(a and b), have values above 10 m/s with a predominance of the southwest direction.

The effect of atmospheric parameters on the adhesion of dirt particles to the surface of PV modules have been studied by several authors [64,66,72,74]. In most cases dust adheres to the surface when the relative humidity exceeds 70 %, regardless of their chemical composition. Nevertheless, in the presence of hygroscopic materials such as gypsum, RH values above 20 % will induce almost instantaneous moisture condensation, increasing the adhesion rate [66]. Gypsum can be partially or completely solubilized depending on the ambient temperature and relative humidity of the environment [75–78]. In the case of the city of Mejillones, nighttime atmospheric conditions, characterized by high levels of relative humidity (above 70 %), allow the partial or total dissolution of the gypsum present on the surface of the PV modules. During daytime hours, the increase in ambient temperature causes the evaporation of the absorbed humidity, which induces the recrystallization of the gypsum in the form of crusts adhered to the surface of the modules. This recrystallization phenomenon acts as a binding agent, cementing dust particles and other environmental contaminants to form compact and highly adherent crusts. A similar phenomenon occurs with calcite, which has the ability to partially or completely dissolve at relative humidities above 70 %. It then recrystallizes to form solid bridges between the powder particles and the glass surface, causing a cementation effect that significantly increases the adhesion of the particulate material [73].

Scanning electron microscopy (SEM) and energy dispersive X-ray (EDX) analyses (Fig. 5) confirm the consolidated structure of these crusts and the incorporation of additional particles into the recrystallised gypsum and calcite matrix. Consequently, the observed soiling on the PV modules of the coal-fired power plant is the result of a cementation process driven by the presence of gypsum and calcite, whose solubility and subsequent recrystallization processes are influenced by local

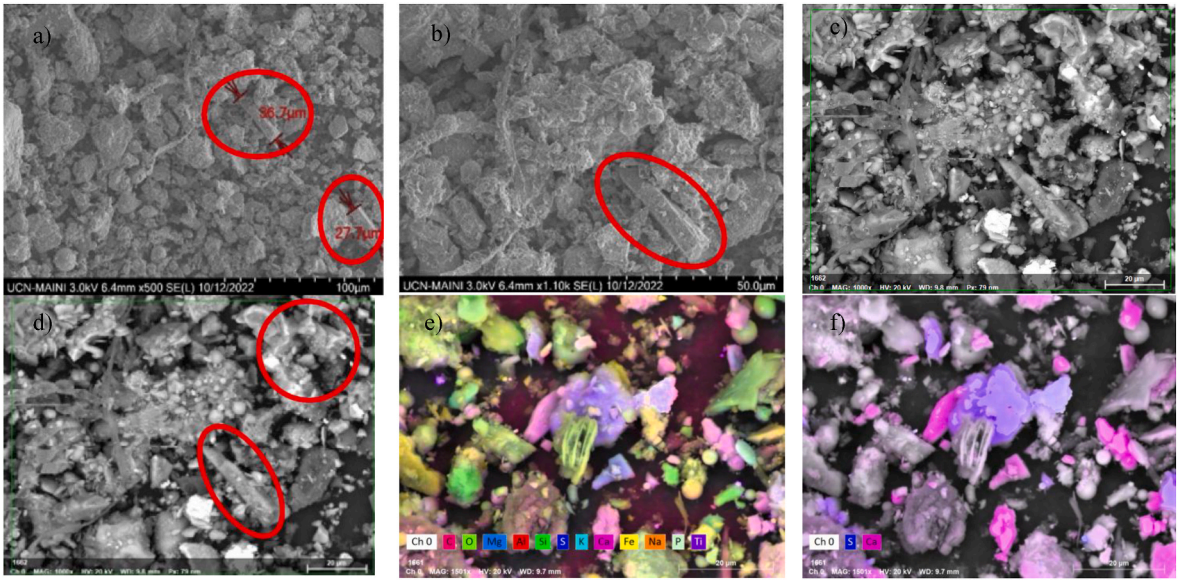


Fig. 5. Scanning Electron Microscopy. a), b), and c) Dust samples collected from the surface of a photovoltaic module installed in a thermoelectric coal-fired power plant. d) Elemental analysis mapping of a random section of the dust samples deposited on photovoltaic modules. e) and f) Sample of soluble material (gypsum) and its capacity to form agglomerates.

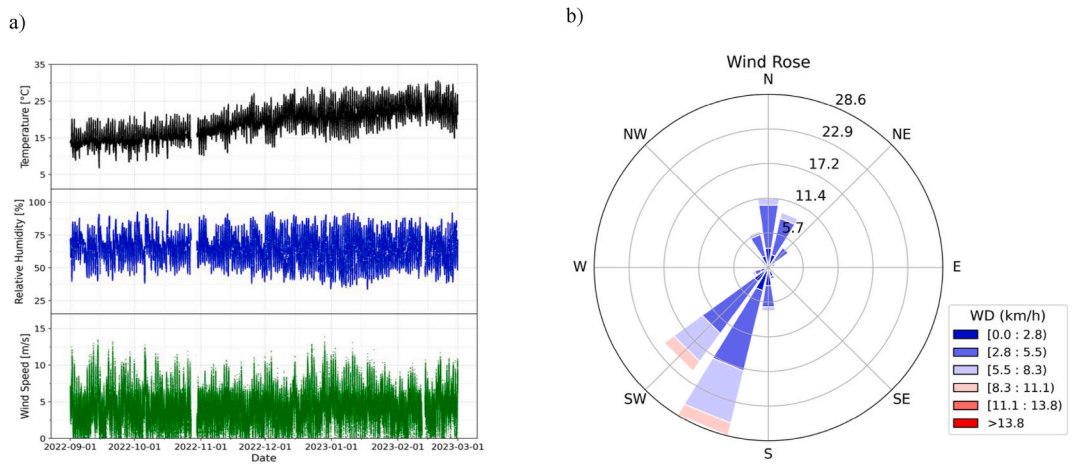


Fig. 6. Parameters atmospheric in the city of Mejillones over a 6-month period (September 2022 to February 2023) included: a) temperature (°C), relative humidity (RH%), wind speed (m/s), and b) wind rose (km/h).

humidity and temperature conditions. These processes allow the formation of solid bridges between the dust particles and the glass surface, resulting in the adhesion of the particulate material.

3.3. The impact of coal-fired power plants on PV plants

The presence of gypsum in this photovoltaic plant is strongly influenced by its proximity to the thermoelectric coal-fired power plant. This type of power plant generates combustion fumes, which consist of a mixture of contaminants such as ashes, unburned particles, and combustion gases like CO_2, SO_2, and NO_X [63]. These gases are treated using desulfurization equipment, with limestone ($CaCO_3$) as the main raw material, in a process known as wet flue gas desulfurization. This compound was detected through the X-ray diffraction analysis (Fig. 3), with a presence of 30 %.

In the desulfurization process, a cycle of chemical reactions occurs in three phases (solid, liquid, and gaseous). The series of reactions that take place in the process was summarized by Neveux et al. [79]. and is shown in Table 1. This process starts when sulphur dioxide (SO_2), a byproduct of combustion gases, is chemically absorbed in an aqueous limestone suspension, forming calcium sulfite ($CaSO_3$), which then reacts with oxygen to generate synthetic gypsum (FDG for flue-desulfurization {gypsum). The efficiency of this process depends on the controlled stages of SO_2 absorption, HSO_3^- oxidation, limestone dissolution, and gypsum crystallization. In the first stage, SO_2 is absorbed in an aqueous solution, allowing the transport of SO_2 in the form of HSO_3^- and SO_3^{-2} [79]. Subsequently, HSO_3^- ions are oxidized to SO_4^{-2} ions in the presence of sufficient O_2. The H^+ ions, produced from the absorption of SO_2 and the oxidation of HSO_3^-, react with limestone particles, producing Ca_2^+ ions. This reaction leads to the formation of semi-hydrated sulfite due to the reactions between Ca_2^+ and HSO_3^- in the aqueous medium, resulting in its precipitation. Finally, synthetic gypsum (FDG) is formed through the reaction of Ca^{2+} ions from limestone dissolution and SO_4^{-2} ions in the oxidation step [80]. Then, the formed synthetic gypsum is removed as residue along with the ashes, which are collected in containers. The transportation of chimney-generated waste to designated storage areas is done through trucks carrying tons of gypsum, ashes, and other contaminants produced during the process. From this point onward, the wind transports these contaminants through the air during the trucks' loading cycles. Thus, the arrow-shaped prisms observed in the SEM images (Fig. 6) and $CaSO_4$ detected through XRD and SEM-EDX correspond to FDG. This combustion residue, with the same properties as natural Gypsum [81], has the main role on the agglomeration and cementation of the deposited material on the surfaces of the photovoltaic modules [82,83].

Table 1
Chemical reactions resulting from desulfurization using wet technology with forced oxidation in thermoelectric coal-fired power plant (based in Neveux et al. [79]).

Stages	Chemical reactions
Absorption of SO_2	$SO_2 + H_2O \leftrightarrow H^+ + HSO_3^-$
	$HSO_3^- \leftrightarrow H^+ + SO_3^{-2}$
Oxidation of HSO_3^-	$HSO_3^- + 0.5\ O_2 \rightarrow H^+ + SO_4^{2-}$
	$H^+ + SO_4^{-2} \leftrightarrow HSO_4^-$
Limestone solution	$CaCO_3 \rightarrow Ca^{+2} + CO_3^{2-}$
	$CO_2 + H_2O \leftrightarrow HCO_3^- + H^+$
	$HCO_3^- \leftrightarrow CO_3^{2-} + H^+$
	$H_2O \leftrightarrow H^+ + OH^-$
Crystallization calcium sulphate semihydrate	$2\ CaCO_3 + H^+ + 2\ HSO_3^- \rightarrow 2\ (CaSO_3 * \frac{1}{2} H_2O) + 2CO_2 + H_2O$
Gypsum crystallization	$Ca^{+2} + SO_4^{-2} + 2\ H_2O \rightarrow CaSO_4 * 2H_2O$
Global reaction	$3CaCO_{3\ (s)} + 3SO_{2\ (g)} + \frac{1}{2} O_{2\ (g)} + 3H_2O_{\ (l)} \rightarrow CaSO_4 * 2H_2O_{\ (s)} + 2CaSO_3 * \frac{1}{2} H_2O_{(s)} + 3CO_{2\ (g)}$

The use of calcite for sulphur dioxide absorption in Chile has been widely adopted, much like in China, where it is used in 90 % of coal-fired power plants, due to its high desulfurization efficiency and low operational cost [63]. This treatment is closely related to regulations aimed to reduce the presence of SO_2 in the atmosphere due to its impact on the environment and human health. However, it is important to consider that this process alters the local geology, producing an impact on the deposition of dirt on nearby PV modules. The coal-fired power plant impacts the environment through the generation of by-products, such as gypsum (FDG), and the use of calcite in the flue gas desulfurization process. This process is designed to reduce SO_2 emissions into the atmosphere. Both synthetic gypsum and calcite interact with the typical dust materials present in the area. Their interaction plays a key role in the cementation process. Gypsum, due to its high hygroscopicity, readily absorbs moisture. Calcite enhances the process by forming solid bridges between dust particles and surfaces. Together, they promote the formation of compact and highly adherent crusts on photovoltaic modules. These crusts significantly increase soiling and make cleaning more challenging. This interaction is not characteristic of the local environment and results in a cementation process that would not occur naturally in the area.

From this process, it is possible to identify the soiling mechanisms that occur in photovoltaic modules. These will be developed in the following stages.

1. Particle deposition: Both the desulfurization byproducts, such as synthetic gypsum (FDG), and the raw material used in this process, calcite, along with other local contaminants, are transported by wind from nearby sources, including industrial emissions and the surrounding desert environment. These particles are deposited on the surface of the photovoltaic module.
2. Dissolution of soluble materials: During the night, when relative humidity exceeds 70 %, soluble materials present in the dust, such as synthetic gypsum (FDG) and calcite, partially or completely dissolve due to moisture condensation on the module surface.
3. Recrystallization and crust formation: At sunrise, as ambient temperature increases, the soluble materials recrystallize, forming compact crusts and solid bridges between dust particles and the glass surface. The consolidated matrix is composed of soluble materials, such as gypsum (FDG) and calcite, along with insoluble materials, such as sand, reinforcing the structure adhered to the module surface.
4. Daily cycle: This cycle of deposition, dissolution, and recrystallization repeats daily, reinforcing dust adhesion and the formation of increasingly resistant and difficult-to-remove cemented layers

To evaluate the impact of the thermoelectric coal-fired power plant on dust deposited on PV modules at nearby plants, XRD analyses and comparisons were performed at different sites: Site 1, a new PV facility located 9 km east of Mejillones; Antofagasta, an urban area located 60 km south of Mejillones; and PSDA, located 120 km southeast of Mejillones (60 km from the coast). The chemical analyses for Antofagasta and PSDA correspond to previously reported data [54,84].

Fig. 7 compares the relative amount of the crystalline species found at each of the four locations. At Site 1, the same compounds than in Mejillones are observed but in different proportions. The main difference regards Calcite, which has the largest presence in Mejillones and a low frequency in Site 1, while quartz and albite have an important presence in both places. Orthoclase, clinochlore and muscovite show similar frequencies at both places, each of them with a presence below 7 %. The presence of gypsum, with a concentration of 2 %, suggests that the coal-fired power plant is generating emissions of FGD gypsum that are transported by the wind, as shown in Fig. 6. Although wind events come mainly from the southwest, opposite the location of the thermoelectric coal-fired power plant, there are wind gusts from the north and northeast that can transport this material. At Antofagasta, a coastal zone like Mejillones, two new compounds are observed, anorthite and halite, while there are no traces of gypsum, clinochlore and muscovite. Particularly, the absence of Gypsum at Antofagasta suggests this material corresponds to a synthetic residue from the coal-fired power plant.

At the PSDA, the same phenomenon of gypsum-induced cementation described for Mejillones occurs [57] but under completely different atmospheric and geological conditions. At Mejillones the presence of gypsum is below 7 % but the average humidity is above 40 %, unlike the PSDA where humidity events are sporadic with low coastal influence, but with gypsum as the main compound (above 50 %). Although gypsum-driven cementation is observed at both installations, these differences affect the impact of soiling on PV energy production, influencing operational and maintenance planning. As a result, cleaning strategies and maintenance intervals must be adjusted based on the accumulated dust density to minimize the impact of soiling on the efficiency and lifespan of the modules at each site.

3.4. Effects of soiling

To assess the impact of soiling resulting from a thermoelectric coal-fired power plant, the surface density of deposited dust was measured over a period of five months in a weekly basis at Mejillones, and monthly at Antofagasta and PSDA. Fig. 8 shows that Mejillones exhibits the largest dust deposition increment reaching a maximum value of 1.8 mg/cm^2 at the end of the experimentation period. Additionally, a self-cleaning phenomenon is observable, occurring between weeks 6–10 and at weeks 15 and 16. Since there was no human intervention, this cleaning effect is attributed to local atmospheric conditions, specifically the condensation of excessive relative humidity due to its coastal location. As shown in Fig. 6b, the city of Mejillones experiences high relative humidity levels, which are adequate to condense ambient relative humidity and trigger a natural cleaning mechanism. However, a residue of contamination, which cannot be naturally removed remains and dirt crusts accumulate [54].

The difficulty in removing the deposited soiling, even under favourable humidity conditions for self-cleaning, is explained by the phenomenon of cementation, which contributes to the formation of desert pavement. In this process, the first layer of cemented material is formed where dirt is initially deposited and has the longest exposure time. As the exposure time increases, this layer becomes an impermeable barrier, and a second layer of material is deposited on top [54]. Finally, a third layer is deposited but its shortest exposure time, allows easy removal through the action of rain, dew, or wind. In the case of the samples exposed to the by-products of the coal-fired power plant and calcite for the desulfurization process, it is observed that the base layer

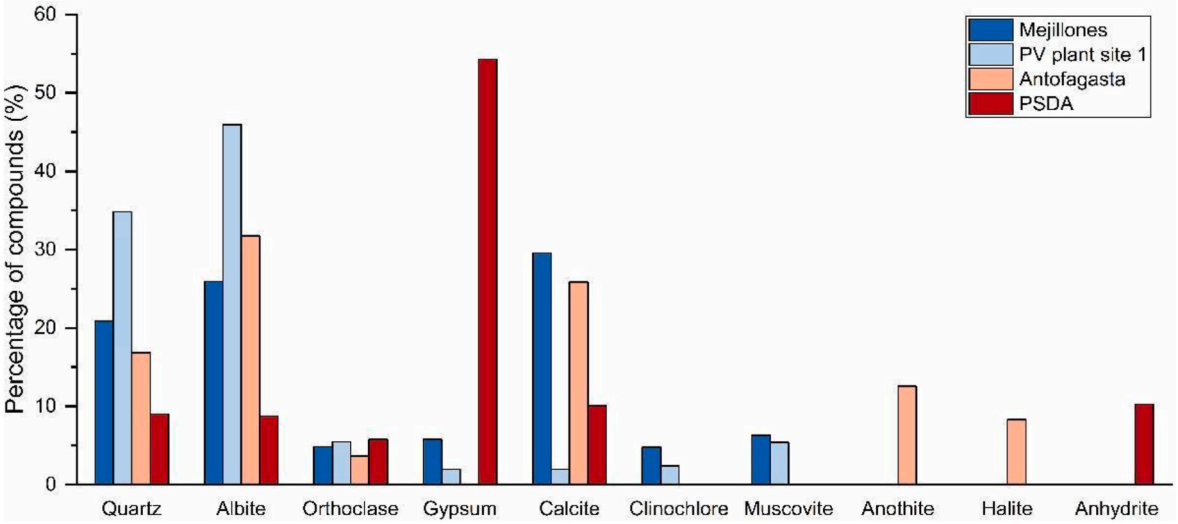


Fig. 7. Comparative graph of crystalline species found in the area of the thermoelectric coal-fired power plant activity in the coastal city of Mejillones, in the Plataforma Solar del Desierto de Atacama (PSDA) in the inner desert [57], the Antofagasta coastal city [56], and at PV plant site 1.

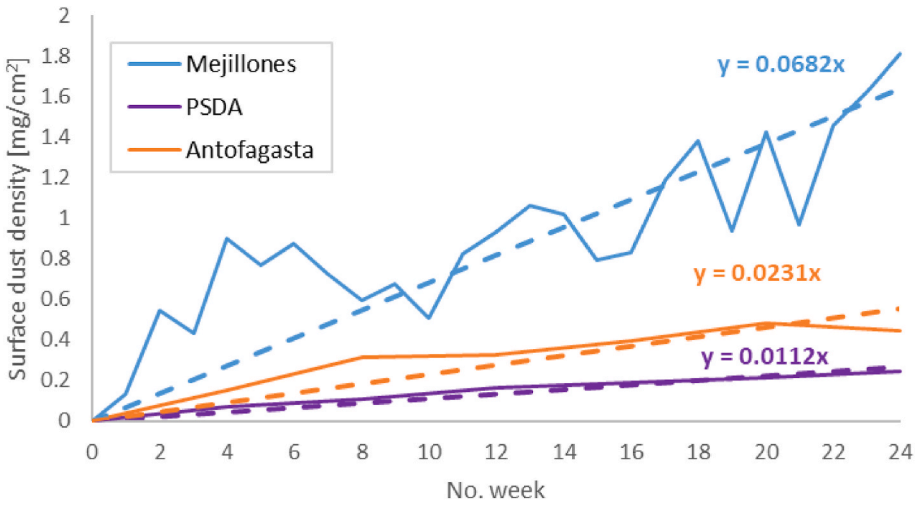


Fig. 8. Surface density of dust deposited on the surface of PV modules installed in Mejillones (blue), where the coal-fired thermoelectric power plant is located, Plataforma solar del Desierto de Atacama (purpure) and Antofagasta city in the coastline (orange) [53] for 5 months of exposure (from September 21, 2022, to February 21, 2023). (For interpretation of the references to colour in this figure legend, the reader is referred to the Web version of this article.)

of dirt is formed in 3 weeks, reaching a density of 0.30 mg/cm^2. Then, this layer serves as a propellant for the generation of the second dirt layer. The (b) type layers are observed in week 10 (0.50 mg/cm^2) and week 15 (0.75 mg/cm^2). Despite evidence of mass losses due to self-cleaning actions (third layer), a baseline soiling is maintained, contributing to the formation of new layers of dirt. This has a significant impact on the cleaning plans of PV plants, since with longer exposure time it becomes much more challenging to remove the dirt crusts. The cemented material causes the particles to be strongly adhered to and cannot be easily removed through standard cleaning methods, such as water washing and brushing. Thus, a more frequent cleaning would be necessary to avoid the use of highly abrasive cleaning methods.

At the PSDA, the deposited dust is significantly lower compared to the industrial environment dominated by the thermoelectric coal-fired power plant. By the end of the experiment, dust density at PSDA (0.2 mg/cm^2) is only 11 % of the 1.8 mg/cm^2 observed in Mejillones. Measurements at Antofagasta (previously reported [53]), show that after 25 weeks of exposure, a maximum of 0.4 mg/cm^2 was deposited. This represents a 78 % reduction compared to Mejillones and a 50 % increase compared to PSDA. A linear fit was made to the results shown in Fig. 8 to obtain an average value for the soiling rate at each one of the three sites. The values obtained were 0.0682, 0.0231 and 0.0112 [mg/cm^2 week] for Mejillones, Antofagasta and PSDA, respectively. The soiling rate at Mejillones was 6 times higher than the inner desert soiling rate at PSDA, and 3 times higher than at Antofagasta, with a coastal climate similar to Mejillones. Thus, the thermoelectric coal-fired power plant has a significant impact on the accumulation of dust, far exceeding the levels of soiling compared to the city of Antofagasta and even more so when compared to the PSDA. Dust accumulation reported for other urban locations, such as Kathmandu (Nepal), the cities of Baduin (Indonesia), and Perth (Western Australia), show significantly lower levels of deposited dust density compared to the coal-powered thermoelectric power plant analysed in this study [85,86]. In Kathmandu, after 5 months the total accumulation was 0.967 mg/cm^2, while after 12 months in Baduin and Perth dust density reached 0.21 mg/cm^2 and 0.28 mg/cm^2, respectively. Comparison of the long-term experiments in these cities with our results for Mejillones highlights the significant impact of the coal-fired thermoelectric power plant on dust accumulation compared to other urban sites.

The transmittance loss due to soiling (τ_{loss}) was evaluated every six weeks at Mejillones (Fig. 9). The largest lost is observed between weeks 12 and 18, which coincide with a significant increment in the deposited material (Fig. 8). Through equations (3) and (4) the effect of soiling on

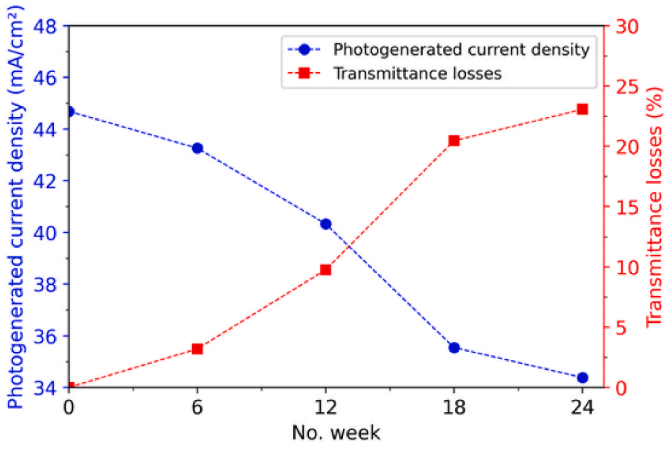


Fig. 9. Transmittance loss due to soiling due to exposure time and theoretical photogenerated current, calculated for a standard P-type cell.

the photogenerated current density (J_{ph}) can be computed from the measured transmittance loss, considering the solar spectral irradiance (ϕ_{in}) and the external quantum efficiency of a specific photovoltaic technology (EQE) [14]. Fig. 9 shows the impact of exposure time to soiling on the photogenerated current density. The initial value of 44.7 mA/cm^2 gradually decays due to the increase in dust density. After 12 weeks of exposure the calculated current density decreases in 4.4 mA/cm^2 due to soiling deposition, followed by a similar decay (4.8 mA/cm^2) but in only 6 weeks. The lowest current, 34.4 mA/cm^2, is observed at week 24 (the last measurement), when the soiling density comes to its maximum value of 1.82 mg/cm^2 and the transmittance loss is of 23.1 %. Thus, the total calculated loss of photogenerated current density is of 23 %, which is larger than the 10 % reported after 12 months of exposure in a suburban area in Madrid (Spain) [87] and the 12 % loss reported in Málaga, a residential/industrial area in Spain, also after 12 months [88]. Nevertheless, higher losses have been reported on the Gran Canarias Island, where optical losses reach 80 % in 5 months in an industrial building construction environment [89].

3.5. Cleaning and maintenance strategies

The PV modules efficiency can be significantly impacted by dust accumulation, especially in arid and desert environments. Determining

the optimal cleaning frequency and methods is crucial for maintaining high power output and minimizing costs [90–94]. In this case, cleaning strategies for PV systems installed near coal-fired power plants must be adapted to the specific characteristics of the environment. Particularly, the presence of by-products of the desulfurization process, such as synthetic gypsum (FDG) and calcite, contribute to the phenomenon of cementation on the module surfaces. These conditions require specific methods to ensure effective cleaning and minimize damage to the module surfaces. In the case of synthetic gypsum (FDG) and calcite, cemented crusts influence the choice of cleaning method between water and dry cleaning.

The use of dry cleaning should be limited to short intervals between cleanings to prevent the formation of cemented crusts containing abrasive particles such as sand. This is particularly important as sand, with a hardness of 7 on the Mohs scale, can damage glass surfaces during mechanical cleaning if the cemented material has not been removed beforehand [95,96]. On the other hand, it is recommended to use water cleaning if the dirt crust has already formed. Water is essential to dissolve crusts formed by soluble materials such as gypsum and calcite. This technique not only removes cemented layers but also crusts formed by soluble materials such as gypsum and calcite [97]. However, the use of water is not a sustainable or recommended solution in desert regions due to its high cost and scarcity [98].Another option may be the use of robotic cleaning technologies. Robotic systems can adapt to specific site conditions and perform scheduled and consistent cleaning, reducing the risk of surface damage and optimising water and energy use [99]. In addition, the use of robots can be particularly useful in preventing the formation of cementation crusts on PV module surfaces, as their constant action prevents soluble materials such as synthetic gypsum (FDG) and calcite from recrystallising and solidifying. This eliminates the need to use water to dissolve the crusts, which is a significant benefit in terms of conserving water resources and reducing operating costs. Similarly, it is crucial to consider the cost-benefit of frequent cleaning in relation to the energy losses caused by soiling. An optimal strategy should balance the cost of cleaning and module maintenance with the reduction of energy generation losses, thereby maximising the operational efficiency of the PV system [94,100–102].

Below is a summary of the recommended cleaning methods for photovoltaic plants located near the influence of a coal-fired power plant (Table 2).

4. Conclusion

This study investigates the influence of a conventional coal-fired power plant on the mechanisms and effects of soiling on photovoltaic (PV) modules, with a particular focus on the products and by-products of the flue gas desulfurization process. This process, implemented to reduce sulphur dioxide (SO_2) emissions to the atmosphere and mitigate its environmental impact, uses calcite as a raw material which reacts with combustion gases producing synthetic gypsum (FDG). Both compounds, gypsum and calcite, play a crucial role in the cementation phenomenon. Gypsum dissolves and recrystallizes under high relative humidity conditions due to its high hygroscopicity, while calcite contributes to cementation by forming solid bridges between dust particles and the glass surface. Over a period of 24 weeks, it was recorded that 1.82 mg/cm^2 of accumulated dust, reduced the optical transmittance by 23 %, which in turn led to a significant decrease of the photogenerated current density, 10.3 mA/cm^2. Dust accumulated due to the coal-fired power plant was 3 times larger compared to other coastal conditions (Antofagasta city), highlighting the importance of implementing specific cleaning and maintenance strategies to mitigate these effects and preserve system performance.

Unlike previous studies, this work demonstrates how synthetic gypsum and calcite, in combination with local atmospheric conditions, significantly influence the composition, adhesion and effect of dust particles on PV module surfaces. This approach provides a new perspective on the impact of industrial emissions on energy efficiency and highlights the need to develop specific mitigation and maintenance strategies. However, some limitations should be acknowledged. This study identifies key soiling compounds and their effects on PV performance but does not fully determine their specific impact on energy efficiency. The analysis focuses on optical transmittance and current density reduction, leaving power output and long-term degradation effects for future research. Additionally, cleaning mechanisms, both natural (e.g., wind, rain) and artificial (e.g., manual, automated), are not explored in depth. Further studies should assess cleaning efficiency and its role in mitigating cementation effects from gypsum and calcite accumulation.

Finally, this study provides an important basis for future research into the impact of industrial emissions on soiling of PV module, highlighting the need to develop specific cleaning strategies and maintenance plans adapted to local conditions. It also highlights the importance of developing adaptive plans under variable atmospheric and industrial conditions to maximise the efficiency and lifetime of PV installations located near industrial activities.

CRediT authorship contribution statement

D. Olivares: Writing – review & editing, Writing – original draft, Validation, Supervision, Resources, Project administration, Methodology, Investigation, Funding acquisition, Formal analysis, Data curation, Conceptualization. **A. Marzo:** Writing – review & editing, Writing – original draft, Visualization, Validation, Supervision, Resources, Methodology, Investigation, Funding acquisition, Formal analysis, Conceptualization. **A. Taquichiri:** Investigation, Formal analysis, Data curation. **R. Espinoza:** Formal analysis, Data curation. **M. Henriquez:** Resources, Funding acquisition. **C. Portillo:** Funding acquisition. **P. Ferrada:** Methodology, Funding acquisition, Conceptualization. **L.A. Conde:** Investigation, Data curation. **E. Fuentealba:** Resources, Funding acquisition. **V. del Campo:** Writing – review & editing, Writing – original draft, Supervision, Resources, Methodology, Investigation, Funding acquisition, Formal analysis, Data curation.

Table 2
Summary of the recommended cleaning methods for photovoltaic plants located near the influence of a coal-fired power plant.

Cleaning Method	Applicable Conditions	Advantages	Disadvantages
Dry Cleaning	Recommended only if performed regularly to prevent material cementation. Not recommended for extended cleaning periods due to the presence of sand, which can scratch the glass surface.	Does not require water	Not effective for removing cemented crusts. May cause scratches on the glass surface. May require more frequent cleaning to prevent dirt accumulation and cementation.
Water Cleaning	Suggested for the presence of cemented crusts, with the aim of dissolving formations caused by soluble material.	Effective in dissolving cemented crusts and removing adhered dirt.	Requires water.
Robotic Cleaning	Recommended to prevent the formation of cemented crusts through scheduled and frequent cleanings. Can operate in site-specific conditions and adapt to environmental needs	Minimizes the need for human intervention. Optimizes water and energy use. Prevents material cementation, reducing the need for water cleaning.	Requires an initial investment in technology and system maintenance. May not be efficient in removing already formed crusts if not used frequently enough.

Declaration of competing interest

The authors declare that they have no known competing financial interests or personal relationships that could have appeared to influence the work reported in this paper.

Acknowledgments

The authors thank Grant RYC2021-031958-I funded by MICIU/AEI/10.13039/501100011033 and by the European Union "NextGenerationEU/PRTR; ANID/FONDAP/1523A0006 "Solar Energy Research Center" SERC-Chile; Chilean Economic Development Agency (CORFO), contract No17PTECES-75830 for project "AtaMoS TeC"; ANID–Fondecyt 1210490, ANID - Millennium Science Initiative Program - NNBP # NCN2021_021. Engineering Project 2030 Code 16ENI2-71940. Unidad de equipamiento científico "MAINI" at Universidad Católica del Norte for supporting sample preparation and data analysis and generation through the XRD and SEM team. The authors want to acknowledge the CACTUS project funded by the European Commission in the HORIZON-INFRA-2023-DEV-01-06 program (Ref.: 101132182). This work was partially done by Aitor Marzo into a visit at the University of Antofagasta, supported by MINEDUC-UA project, code ANT22991.

References

[1] I.P. on C.C. (IPCC), Health, wellbeing and the changing structure of communities, climate change 2022 – impacts, adaptation and vulnerability, 1041–1170, https://doi.org/10.1017/9781009325844.009, 2023.
[2] D. jones, S. Brown, P. Czyzak, European electricity review 2023 | ember. https://ember-climate.org/insights/research/european-electricity-review-2023/, 2023. (Accessed 1 April 2024).
[3] IRENA, RENEWABLE CAPACITY STATISTICS 2021, International Renewable Energy Agency (IRENA), Abu Dhabi, 2021. www.irena.org.
[4] Solar Power Europe, Global market outlook 2023-2027. http://www.solarpowereurope.org/insights/global-market-outlook/, 2023. (Accessed 7 March 2024).
[5] P. Bórawski, L. Holden, A. Bełdycka-Bórawska, Perspectives of photovoltaic energy market development in the European Union, Energy 270 (2023) 126804, https://doi.org/10.1016/J.ENERGY.2023.126804.
[6] M. Victoria, N. Haegel, I.M. Peters, R. Sinton, A. Jäger-Waldau, C. del Cañizo, C. Breyer, M. Stocks, A. Blakers, I. Kaizuka, K. Komoto, A. Smets, Solar photovoltaics is ready to power a sustainable future, Joule 5 (2021) 1041–1056, https://doi.org/10.1016/J.JOULE.2021.03.005.
[7] E. Vartiainen, G. Masson, C. Breyer, D. Moser, E. Román Medina, Impact of weighted average cost of capital, capital expenditure, and other parameters on future utility-scale PV levelised cost of electricity, Prog. Photovoltaics Res. Appl. 28 (2020) 439–453, https://doi.org/10.1002/PIP.3189.
[8] ASTM D4728 IEC 60068 Composite Salt Spray Test Machine - LISUN, (n.d.). https://www.lisungroup.com/products/environmental-test-chamber/composite-salt-spray-test-chamber.html (accessed February 1, 2025).
[9] M. Trigo-González, M. Cortés-Carmona, A. Marzo, J. Alonso-Montesinos, M. Martínez-Durbán, G. López, C. Portillo, F.J. Batlles, Photovoltaic power electricity generation nowcasting combining sky camera images and learning supervised algorithms in the Southern Spain, Renew. Energy 206 (2023) 251–262, https://doi.org/10.1016/J.RENENE.2023.01.111.
[10] A. Salmon, A. Marzo, J. Polo, J. Ballestrín, E. Carra, J. Alonso-Montesinos, World map of low-layer atmospheric extinction values for solar power tower plants projects, Renew. Energy 201 (2022) 876–888, https://doi.org/10.1016/j.renene.2022.11.003.
[11] P. Ferrada, A. Marzo, M. Ruiz Ferrández, E. Ruiz Reina, B. Ivorra, J. Correa-Puerta, V. del Campo, Optimization of N-PERT solar cell under Atacama Desert solar spectrum. https://doi.org/10.3390/nano12203554, 2022.
[12] J.F. Lelièvre, R. Couderc, N. Pinochet, L. Sicot, D. Munoz, R. Kopecek, P. Ferrada, A. Marzo, D. Olivares, F. Valencia, E. Urrejola, Desert label development for improved reliability and durability of photovoltaic modules in harsh desert conditions, Solar Energy Materials and Solar Cells 236 (2022) 111508. https://doi.org/10.1016/J.SOLMAT.2021.111508.
[13] D. Olivares, P. Ferrada, A. Marzo, J. Llanos, C. Miranda-Ostojic, V. del Campo, S. Bravo, E. Fuentealba, Microstructural analysis of the PV module cementation process at the solar platform of the Atacama Desert, Sol. Energy Mater. Sol. Cell. 227 (2021), https://doi.org/10.1016/j.solmat.2021.111109.
[14] P. Ferrada, A. Marzo, E. Cabrera, H. Chu, V. del Campo, J. Rabanal, D. Diaz-Almeida, A. Schneider, R. Kopecek, Potential for photogenerated current for silicon based photovoltaic modules in the Atacama Desert, Sol. Energy 144 (2017) 580–593, https://doi.org/10.1016/j.solener.2017.01.053.
[15] J. Ballestrín, J. Polo, N. Martín-Chivelet, J. Barbero, E. Carra, J. Alonso-Montesinos, A. Marzo, Soiling forecasting of solar plants: a combined heuristic approach and autoregressive model, Energy 239 (2022) 122442, https://doi.org/10.1016/J.ENERGY.2021.122442.
[16] J. Polo, N. Martín-Chivelet, C. Sanz-Saiz, J. Alonso-Montesinos, G. López, M. Alonso-Abella, F.J. Battles, A. Marzo, N. Hanrieder, Modeling soiling losses for rooftop PV systems in suburban areas with nearby forest in Madrid, Renew Energy 178 (2021) 420–428. https://doi.org/10.1016/J.RENENE.2021.06.085.
[17] P. Ferrada, D. Olivares, V. del Campo, A. Marzo, F. Araya, E. Cabrera, J. Llanos, J. Correa-Puerta, C. Portillo, D. Román Silva, M. Trigo-Gonzalez, J. Alonso-Montesinos, G. López, J. Polo, F.J.F.J. Batlles, E. Fuentealba, Physicochemical characterization of soiling from photovoltaic facilities in arid locations in the Atacama Desert, Sol. Energy 187 (2019) 47–56, https://doi.org/10.1016/J.SOLENER.2019.05.034.
[18] K. Ilse, L. Micheli, B.W. Figgis, K. Lange, D. Daßler, H. Hanifi, F. Wolfertstetter, V. Naumann, C. Hagendorf, R. Gottschalg, J. Bagdahn, Techno-economic assessment of soiling losses and mitigation strategies for solar power generation, Joule 3 (2019) 2303–2321, https://doi.org/10.1016/j.joule.2019.08.019.
[19] M.R. Maghami, H. Hizam, C. Gomes, M.A. Radzi, M.I. Rezadad, S. Hajighorbani, Power loss due to soiling on solar panel: a review, Renew. Sustain. Energy Rev. 59 (2016) 1307–1316. http://www.sciencedirect.com/science/article/pii/S1364032116000745. (Accessed 26 March 2017).
[20] B. Figgis, A. Ennaoui, S. Ahzi, Y. Rémond, Review of PV soiling particle mechanics in desert environments, Renew. Sustain. Energy Rev. 76 (2017) 872–881, https://doi.org/10.1016/j.rser.2017.03.100.
[21] B. Figgis, B. Brophy, PV coatings and particle adhesion forces PV coatings and particle adhesion forces, in: Conference Proceedings PV-Days Halle Germany 20, 2015.
[22] K. Ilse, M. Werner, V. Naumann, B.W. Figgis, C. Hagendorf, J. Bagdahn, Microstructural analysis of the cementation process during soiling on glass surfaces in arid and semi-arid climates, Phys. Status Solidi Rapid Res. Lett. 10 (2016) 525–529, https://doi.org/10.1002/pssr.201600152.
[23] D. Olivares, P. Ferrada, A. Marzo, K. Pinto, D. Espinoza, J. Rabanal-Arabach, C. Portillo, E. Fuentealba, J. Llanos, Study of the effects of soiling on PV devices using the spin-coating technique in accelerated indoor exposures, Sol. Energy 231 (2022) 317–327, https://doi.org/10.1016/j.solener.2021.11.036.
[24] P. Borah, L. Micheli, N. Sarmah, Analysis of soiling loss in photovoltaic modules: a review of the impact of atmospheric parameters, soil properties, and mitigation approaches, Sustainability 15 (2023) 16669, https://doi.org/10.3390/SU152416669, 16669 15 (2023).
[25] J.G. Bessa, L. Micheli, F. Almonacid, E.F. Fernández, Monitoring photovoltaic soiling: assessment, challenges, and perspectives of current and potential strategies, iScience 24 (2021) 102165, https://doi.org/10.1016/J.ISCI.2021.102165.
[26] C. Schill, A. Anderson, C. Baldus-Jeursen, L. Burnham, L. Micheli, D. Parlevliet, E. Pilat, B. Stridh, E. Urrejola, IEA PVPS task 13. Performance, operation and reliability of photovoltaic systems. Soiling Losses Impact on the Performance of Photovoltaic Power Plants, 2022, 2022. Report IEA-PVPS T13-21, https://iea-pvps.org/research-tasks/performance-operation.
[27] Á. Fernández-Solas, J. Montes-Romero, L. Micheli, F. Almonacid, E.F. Fernández, Estimation of soiling losses in photovoltaic modules of different technologies through analytical methods, Energy 244 (2022) 123173, https://doi.org/10.1016/J.ENERGY.2022.123173.
[28] R.R. Cordero, A. Damiani, D. Laroze, S. MacDonell, J. Jorquera, E. Sepúlveda, S. Feron, P. Llanillo, F. Labbe, J. Carrasco, J. Ferrer, G. Torres, Effects of soiling on photovoltaic (PV) modules in the Atacama Desert, Sci. Rep. 8 (2018) 13943, https://doi.org/10.1038/s41598-018-32291-8.
[29] D. Olivares, M. Trigo-González, A. Marzo, P. Ferrada, J. Llanos, F. Araya, G. López, J. Polo, J. Alonso-Montesinos, C. Gueymard, Analysis of the local factors that influence the cementation of soil and effects on PV generation at the plataforma solar del desierto de atacama, Chile, in: Proceedings of the ISES Solar World Congress 2019 and IEA SHC International Conference on Solar Heating and Cooling for Buildings and Industry 2019, International Solar Energy Society, 2020, pp. 1051–1060, https://doi.org/10.18086/swc.2019.19.08.
[30] D. Olivares, P. Ferrada, J. Bijman, S. Rodríguez, M. Trigo-González, A. Marzo, J. Rabanal-Arabach, J. Alonso-Montesinos, F.J. Batlles, E. Fuentealba, Determination of the soiling impact on photovoltaic modules at the coastal area of the Atacama Desert, Energies 13 (2020) 3819, https://doi.org/10.3390/en13153819.
[31] D. Olivares, A. Marzo, J. Llanos, P. Ferrada, M. Henríquez, C. Portillo, A. Taquichiri, E. Fuentealba, Impact of soiling physicochemistry on mirrors with CSP applications at the plataforma solar del desierto de atacama, Chile, in: SolarPACES Conference Proceedings, vol. 1, 2022, https://doi.org/10.52825/SOLARPACES.V1I.738.
[32] G.P. Smestad, T.A. Germer, H. Alrashidi, E.F. Fernández, S. Dey, H. Brahma, N. Sarmah, A. Ghosh, N. Sellami, I.A.I. Hassan, M. Desouky, A. Kasry, B. Pesala, S. Sundaram, F. Almonacid, K.S. Reddy, T.K. Mallick, L. Micheli, Modelling photovoltaic soiling losses through optical characterization, Sci. Rep. 10 (1) (2020) 1–13, https://doi.org/10.1038/s41598-019-56868-z, 10 (2020).
[33] M.M. Fraga, B.L. de O. Campos, T.B. de Almeida, J.M.F. da Fonseca, V. de F. C. Lins, Analysis of the soiling effect on the performance of photovoltaic modules on a soccer stadium in Minas Gerais, Brazil, Sol. Energy 163 (2018) 387–397, https://doi.org/10.1016/J.SOLENER.2018.02.025.
[34] A. Zeedan, A. Barakeh, K. Al-Fakhroo, F. Touati, A.S.P. Gonzales, Quantification of PV power and economic losses due to soiling in Qatar, Sustainability 13 (2021) 3364, https://doi.org/10.3390/SU13063364, 3364 13 (2021).
[35] P. Ferrada, F. Araya, A. Marzo, E. Fuentealba, Performance analysis of photovoltaic systems of two different technologies in a coastal desert climate zone of Chile, Sol. Energy 114 (2015) 356–363, https://doi.org/10.1016/j.solener.2015.02.009.

[36] E. Fuentealba, P. Ferrada, F. Araya, A. Marzo, C. Parrado, C. Portillo, Photovoltaic performance and LCoE comparison at the coastal zone of the Atacama Desert, Chile, Energy Convers. Manag. 95 (2015) 181–186, https://doi.org/10.1016/j.enconman.2015.02.036.
[37] K.K. Ilse, B.W. Figgis, V. Naumann, C. Hagendorf, J. Bagdahn, Fundamentals of soiling processes on photovoltaic modules, Renew. Sustain. Energy Rev. 98 (2018) 239–254, https://doi.org/10.1016/J.RSER.2018.09.015.
[38] K.K. Ilse, B.W. Figgis, M. Werner, V. Naumann, C. Hagendorf, H. Pöllmann, J. Bagdahn, Comprehensive analysis of soiling and cementation processes on PV modules in Qatar, Sol. Energy Mater. Sol. Cell. 186 (2018) 309–323, https://doi.org/10.1016/J.SOLMAT.2018.06.051.
[39] S. Mills, Combining solar power with coal-fired power plants, or cofiring natural gas, Clean Energy 2 (2018) 1–9, https://doi.org/10.1093/CE/ZKY004.
[40] M. Jiang, Y. Lv, T. Wang, Z. Sun, J. Liu, X. Yu, J. Yan, Performance analysis of a photovoltaics aided coal-fired power plant, Energy Proc. 158 (2019) 1348–1353, https://doi.org/10.1016/J.EGYPRO.2019.01.330.
[41] J.L. Fan, M. Xu, L. Yang, X. Zhang, Benefit evaluation of investment in CCS retrofitting of coal-fired power plants and PV power plants in China based on real options, Renew. Sustain. Energy Rev. 115 (2019) 109350, https://doi.org/10.1016/J.RSER.2019.109350.
[42] H. Yan, X. Li, M. Liu, D. Chong, J. Yan, Performance analysis of a solar-aided coal-fired power plant in off-design working conditions and dynamic process, Energy Convers. Manag. 220 (2020) 113059, https://doi.org/10.1016/J.ENCONMAN.2020.113059.
[43] H. Liu, R. Zhai, K. Patchigolla, P. Turner, Y. Yang, Performance analysis of a novel combined solar trough and tower aided coal-fired power generation system, Energy 201 (2020) 117597, https://doi.org/10.1016/J.ENERGY.2020.117597.
[44] C. Haiping, Z. Heng, B. Yuegang, L. Haowen, Z. Xuelei, The performance analysis and evaluation of C-PV/T aided power generation system, Int. J. Energy Res. 42 (2018) 863–876, https://doi.org/10.1002/ER.3833.
[45] K. Bódis, I. Kougias, N. Taylor, A. Jäger-Waldau, Solar photovoltaic electricity generation: a lifeline for the European coal regions in transition, Sustainability 11 (2019) 3703, https://doi.org/10.3390/SU11133703, 3703 11 (2019).
[46] C. Serrano-Sanchez, M. Olmeda-Delgado, F. Petrakopoulou, Exergy and economic evaluation of a hybrid power plant coupling coal with solar energy, Appl. Sci. 9 (2019) 850, https://doi.org/10.3390/APP9050850, 850 9 (2019).
[47] H. Hong, S. Peng, Y. Zhao, Q. Liu, H. Jin, A typical solar-coal hybrid power plant in China, Energy Proc. 49 (2014) 1777–1783, https://doi.org/10.1016/J.EGYPRO.2014.03.188.
[48] P. Córdoba, P. Córdoba, Emissions of inorganic trace pollutants from coal power generation, air pollution - monitoring. Quantification and Removal of Gases and Particles, 2018, https://doi.org/10.5772/INTECHOPEN.79918.
[49] A. Zurita, C. Mata-Torres, C. Valenzuela, C. Felbol, J.M. Cardemil, A.M. Guzmán, R.A. Escobar, Techno-economic evaluation of a hybrid CSP + PV plant integrated with thermal energy storage and a large-scale battery energy storage system for base generation, Sol. Energy 173 (2018) 1262–1277, https://doi.org/10.1016/j.solener.2018.08.061.
[50] S. Carver, N. Mikkelsen, J. Woodward, Long-term rates of mass wasting in Mesters Vig, northeast Greenland: notes on a re-survey, Permafr. Periglac. Process. (2002), https://doi.org/10.1002/ppp.421.
[51] M. Kottek, J. Grieser, C. Beck, B. Rudolf, F. Rubel, World map of the Köppen-Geiger climate classification updated, Meteorol. Z. 15 (2006) 259–263, https://doi.org/10.1127/0941-2948/2006/0130.
[52] M. Concha, G.A. Ruz, Evaluation of atmospheric environmental regulations: the case of thermoelectric power plants, Atmosphere (2023), https://doi.org/10.3390/atmos14020358 (Basel).
[53] D. Olivares, P. Ferrada, J. Bijman, S. Rodríguez, M. Trigo-González, A. Marzo, J. Rabanal-Arabach, J. Alonso-Montesinos, F.J. Batlles, E. Fuentealba, Determination of the soiling impact on photovoltaic modules at the coastal area of the Atacama Desert, Energies 13 (2020) 1–17, https://doi.org/10.3390/en13153819.
[54] D. Olivares, A. Taquichiri, P. Ferrada, A. Marzo, M. Henríquez, D. Espinoza, E. Fuentealba, J. Llanos, Soil characterization and soiling impact to facilitate photovoltaic installation, Appl. Sci. 12 (2022), https://doi.org/10.3390/app122010582.
[55] S.N. Kabekkodu, J. Faber, T. Fawcett, New Powder Diffraction File (PDF-4) in relational database format: advantages and data-mining capabilities, Acta Crystallogr. B 58 (2002) 333–337, https://doi.org/10.1107/s0108768102002458.
[56] P. Ferrada, D. Olivares, V. del Campo, A. Marzo, F. Araya, E. Cabrera, J. Llanos, J. Correa-Puerta, C. Portillo, D. Román Silva, M. Trigo-Gonzalez, J. Alonso-Montesinos, G. López, J. Polo, F.J. Batlles, E. Fuentealba, Physicochemical characterization of soiling from photovoltaic facilities in arid locations in the Atacama Desert, Sol. Energy 187 (2019) 47–56, https://doi.org/10.1016/j.solener.2019.05.034.
[57] D. Olivares, P. Ferrada, A. Marzo, J. Llanos, C. Miranda-Ostojic, V. del Campo, S. Bravo, E. Fuentealba, Microstructural analysis of the PV module cementation process at the solar platform of the Atacama Desert, Solar Energy Materials and Solar Cells nn (2021), https://doi.org/10.1016/j.solmat.2021.111109.
[58] L. Linzhu, M. Iskander, Evaluation of roundness parameters in use for sand, J. Geotech. Geoenviron. Eng. 147 (2021).
[59] B. Aïssa, R.J. Isaifan, V.E. Madhavan, A.A. Abdallah, Structural and physical properties of the dust particles in Qatar and their influence on the PV panel performance, Sci. Rep. 6 (1) (2016) 1–12, https://doi.org/10.1038/srep31467, 6 (2016).
[60] Portal de Servicios Climáticos - Dirección Meteorológica de Chile, Dirección Metereológia de Chile, 2020.
[61] G. Ureta, K. Németh, F. Aguilera, M. Vilches, M. Aguilera, I. Torres, J. P. Sepúlveda, A. Scheinost, R. González, An overview of the mafic and felsic monogenetic neogene to quaternary volcanism in the central andes, northern Chile (18-28°Lat.S), in: K. Németh (Ed.), IntechOpen, Rijeka, 2020, https://doi.org/10.5772/intechopen.93959. Ch. 11.
[62] A. Binnie, T.J. Dunai, S.A. Binnie, P. Victor, G. González, A. Bolten, Accelerated late quaternary uplift revealed by 10Be exposure dating of marine terraces, Mejillones Peninsula, northern Chile, Quat. Geochronol. 36 (2016) 12–27, https://doi.org/10.1016/j.quageo.2016.06.005.
[63] C. Liu, Q. Zhao, Y. Wang, P. Shi, M. Jiang, Hydrothermal synthesis of calcium sulfate whisker from flue gas desulfurization gypsum, Chin. J. Chem. Eng. 24 (2016) 1552–1560, https://doi.org/10.1016/j.cjche.2016.04.024.
[64] B. Figgis, A. Nouviaire, Y. Wubulikasimu, W. Javed, B. Guo, A. Ait-Mokhtar, R. Belarbi, S. Ahzi, Y. Rémond, A. Ennaoui, Investigation of factors affecting condensation on soiled PV modules, Sol. Energy 159 (2018) 488–500, https://doi.org/10.1016/j.solener.2017.10.089.
[65] D. Olivares, M. Trigo-González, A. Marzo, P. Ferrada, J. Llanos, F. Araya, G. López, J. Polo, J. Alonso-Montesinos, C. Gueymard, Analysis of the local factors that influence the cementation of soil and effects on PV generation at the plataforma solar del desierto de atacama, Chile. Proceedings ISES Solar World Congress 2019, 2019, https://doi.org/10.18086/swc.2019.19.08.
[66] A.P. Bateman, H. Belassein, S.T. Martin, Impactor apparatus for the study of particle rebound: relative humidity and capillary forces, Aerosol. Sci. Technol. 48 (2014) 42–52, https://doi.org/10.1080/02786826.2013.853866.
[67] B. Figgis, A. Ennaoui, S. Ahzi, Y. Remond, Review of PV soiling measurement methods. Proceedings of 2016 International Renewable and Sustainable Energy Conference, IRSEC 2016, 2017, https://doi.org/10.1109/IRSEC.2016.7984027.
[68] K.K. Ilse, B.W. Figgis, V. Naumann, C. Hagendorf, J. Bagdahn, Fundamentals of soiling processes on photovoltaic modules, Renew. Sustain. Energy Rev. 98 (2018) 239–254, https://doi.org/10.1016/j.rser.2018.09.015.
[69] W. Javed, Y. Wubulikasimu, B. Figgis, B. Guo, Characterization of dust accumulated on photovoltaic panels in Doha, Qatar, Sol. Energy 142 (2017) 123–135, https://doi.org/10.1016/j.solener.2016.11.053.
[70] E. Kim, D. Kalman, T. Larson, Dry deposition of large , airborne particles onto a surrogate surface, Atmos. Environ. 34 (2000) 2387–2397, https://doi.org/10.1016/S1352-2310(99)00444-6.
[71] F. Wang, G. Michalski, J. hye Seo, W. Ge, Geochemical, isotopic, and mineralogical constraints on atmospheric deposition in the hyper-arid Atacama Desert, Chile, Geochem. Cosmochim. Acta 135 (2014) 29–48, https://doi.org/10.1016/J.GCA.2014.03.017.
[72] P. Winkler, Relative humidity and the adhesion of atmospheric particles to the plates of impactors, J. Aerosol Sci. (1974), https://doi.org/10.1016/0021-8502(74)90058-5.
[73] K.K. Ilse, B.W. Figgis, M. Werner, V. Naumann, C. Hagendorf, H. Pöllmann, J. Bagdahn, Comprehensive analysis of soiling and cementation processes on PV modules in Qatar, Sol. Energy Mater. Sol. Cell. 186 (2018) 309–323, https://doi.org/10.1016/j.solmat.2018.06.051.
[74] Q. Ma, H. He, Y. Liu, C. Liu, V.H. Grassian, Heterogeneous and multiphase formation pathways of gypsum in the atmosphere, Phys. Chem. Chem. Phys. (2013), https://doi.org/10.1039/c3cp53424c.
[75] A. Watson, Desert gypsum crusts as palaeoenvironmental indicators: a micropetrographic study of crusts from southern Tunisia and the central Namib Desert, J. Arid Environ. (1988), https://doi.org/10.1016/s0140-1963(18)31002-4.
[76] A. Watson, Gypsum crusts in deserts, J. Arid Environ. (1979), https://doi.org/10.1016/s0140-1963(18)31700-31702.
[77] D. Olivares, P. Ferrada, A. Marzo, J. Llanos, C. Miranda-Ostojic, V. del Campo, S. Bravo, E. Fuentealba, Microstructural analysis of the PV module cementation process at the solar platform of the Atacama Desert, Sol. Energy Mater. Sol. Cell. 227 (2021) 111109, https://doi.org/10.1016/j.solmat.2021.111109.
[78] D. Olivares, M. Trigo-González, A. Marzo, P. Ferrada, J. Llanos, F. Araya, G. López, J. Polo, J. Alonso-Montesinos, C. Gueymard, Analysis of the local factors that influence the cementation of soil and effects on PV generation at the plataforma solar del desierto de atacama, Chile. Proceedings of the ISES Solar World Congress 2019 and IEA SHC International Conference on Solar Heating and Cooling for Buildings and Industry 2019, 2020, pp. 1051–1060, https://doi.org/10.18086/swc.2019.19.08.
[79] T. Neveux, Y. Le Moullec, Wet industrial flue gas desulfurization unit: model development and validation on industrial data, Ind. Eng. Chem. Res. 50 (2011) 7579–7592, https://doi.org/10.1021/ie102239q.
[80] J. Lim, Y. Choi, G. Kim, J. Kim, Modeling of the wet flue gas desulfurization system to utilize low-grade limestone, Kor. J. Chem. Eng. 37 (2020) 2085–2093, https://doi.org/10.1007/s11814-020-0639-6.
[81] M. Sandoval, C. Quezada, J. Celis, J.M. Recio, J. Capulín, Potential uso del yeso sintético (fdg) En La agricultura como enmienda en suelos con problemas de salinidad use of synthetic gypsum (Fdg) in agriculture as an amendment of soils with salinity problems, Anim. Sci., Ex Agro-Ciencia 32 (2016) 4–12.
[82] E. Álvarez-Ayuso, X. Querol, A. Tomás, Environmental impact of a coal combustion-desulphurisation plant: abatement capacity of desulphurisation process and environmental characterisation of combustion by-products, Chemosphere 65 (2006) 2009–2017, https://doi.org/10.1016/j.chemosphere.2006.06.070.
[83] B. Guan, H. Fu, J. Yu, G. Jiang, B. Kong, Z. Wu, Direct transformation of calcium sulfite to α-calcium sulfate hemihydrate in a concentrated Ca-Mg-Mn chloride

solution under atmospheric pressure, Fuel 90 (2011) 36–41, https://doi.org/10.1016/j.fuel.2010.08.020.
[84] D. Olivares, P. Ferrada, C. De Matos, A. Marzo, E. Cabrera, C. Portillo, J. Llanos, Characterization of soiling on PV modules in the Atacama Desert, Energy Proc. 124 (2017) 547–553, https://doi.org/10.1016/j.egypro.2017.09.263.
[85] B.R. Paudyal, S.R. Shakya, Dust accumulation effects on efficiency of solar PV modules for off grid purpose: a case study of Kathmandu, Sol. Energy 135 (2016) 103–110, https://doi.org/10.1016/J.SOLENER.2016.05.046.
[86] J. Tanesab, D. Parlevliet, J. Whale, T. Urmee, The effect of dust with different morphologies on the performance degradation of photovoltaic modules, Sustain. Energy Technol. Assessments 31 (2019) 347–354, https://doi.org/10.1016/J.SETA.2018.12.024.
[87] J. Polo, N. Martín-Chivelet, C. Sanz-Saiz, J. Alonso-Montesinos, G. López, M. Alonso-Abella, F.J. Battles, A. Marzo, N. Hanrieder, Modeling soiling losses for rooftop PV systems in suburban areas with nearby forest in Madrid, Renew. Energy 178 (2021) 420–428, https://doi.org/10.1016/j.renene.2021.06.085.
[88] M. Piliougine, C. Cañete, R. Moreno, J. Carretero, J. Hirose, S. Ogawa, M. Sidrach-de-Cardona, Comparative analysis of energy produced by photovoltaic modules with anti-soiling coated surface in arid climates, Appl. Energy (2013), https://doi.org/10.1016/j.apenergy.2013.01.048.
[89] C. Schill, S. Brachmann, M. Koehl, Impact of soiling on IV-curves and efficiency of PV-modules, Sol. Energy 112 (2015) 259–262, https://doi.org/10.1016/j.solener.2014.12.003.
[90] G. Sánchez-Barroso, J. González-Domínguez, J. García-Sanz-Calcedo, J.G. Sanz, Markov chains estimation of the optimal periodicity for cleaning photovoltaic panels installed in the dehesa, Renew. Energy 179 (2021) 537–549, https://doi.org/10.1016/J.RENENE.2021.07.075.
[91] A.H. Shah, A. Hassan, M.S. Laghari, A. Alraeesi, The influence of cleaning frequency of photovoltaic modules on power losses in the desert climate, Sustainability 12 (2020) 9750, https://doi.org/10.3390/SU12229750, 9750 12 (2020).
[92] P.M. Rodrigo, S. Gutiérrez, L. Micheli, E.F. Fernández, F.M. Almonacid, Optimum cleaning schedule of photovoltaic systems based on levelised cost of energy and case study in central Mexico, Sol. Energy 209 (2020) 11–20, https://doi.org/10.1016/J.SOLENER.2020.08.074.
[93] Y. Jiang, L. Lu, H. Lu, A novel model to estimate the cleaning frequency for dirty solar photovoltaic (PV) modules in desert environment, Sol. Energy 140 (2016) 236–240, https://doi.org/10.1016/J.SOLENER.2016.11.016.
[94] M. Al-Housani, Y. Bicer, M. Koç, Assessment of various dry photovoltaic cleaning techniques and frequencies on the power output of CdTe-type modules in dusty environments, Sustainability 11 (2019) 2850, https://doi.org/10.3390/SU11102850. Page 2850 11 (2019).
[95] M.E. Broz, R.F. Cook, D.L. Whitney, Microhardness, toughness, and modulus of Mohs scale minerals, Am. Mineral. 91 (2006) 135–142, https://doi.org/10.2138/AM.2006.1844.
[96] D. Tabor, Mohs's hardness scale - a physical interpretation, Proc. Phys. Soc. B 67 (1954) 249.
[97] A.E. Charola, J. Pühringer, M. Steiger, Gypsum: a review of its role in the deterioration of building materials, Environ. Geol. 52 (2007) 207–220, https://doi.org/10.1007/S00254-006-0566-9/METRICS.
[98] B. He, H. Lu, C. Zheng, Y. Wang, Characteristics and cleaning methods of dust deposition on solar photovoltaic modules-A review, Energy 263 (2023), https://doi.org/10.1016/j.energy.2022.126083.
[99] J. Farrokhi Derakhshandeh, R. AlLuqman, S. Mohammad, H. AlHussain, G. AlHendi, D. AlEid, Z. Ahmad, A comprehensive review of automatic cleaning systems of solar panels, Sustain. Energy Technol. Assessments 47 (2021), https://doi.org/10.1016/j.seta.2021.101518.
[100] M. Naeem, G. Tamizhmani, Cleaning frequency optimization for soiled photovoltaic modules. 2015 IEEE 42nd Photovoltaic Specialist Conference, PVSC, 2015, https://doi.org/10.1109/PVSC.2015.7355972, 2015.
[101] M. Mohamed, M.A. Attia, A.M. Asim, A.Y. Abdelaziz, N. Kanwar, Optimization of cleaning frequency and dust accumulation effect on photovoltaic panels, J. Interdiscipl. Math. 23 (2020) 53–68, https://doi.org/10.1080/09720502.2020.1721658.
[102] D.L. Alvarez, A.S. Al-Sumaiti, S.R. Rivera, Estimation of an optimal PV panel cleaning strategy based on both annual radiation profile and module degradation, IEEE Access 8 (2020) 63832–63839, https://doi.org/10.1109/ACCESS.2020.2983322.